

Original article

Influence of micro-particles on gas hydrate formation kinetics: Potential application to methane storage and transportation

Qiong Wu^{1,2}, Teng Tang¹, Zhiwei Zhao¹, Li Li², Maged Elhefnawey^{2,3}, Baoyong Zhang^{1*}

¹Department of Safety Engineering, Heilongjiang University of Science and Technology, Harbin 150022, P. R. China

²International Joint Laboratory of Advanced Nanomaterials of Heilongjiang Province (International Cooperation), Harbin 150001, P. R. China

³Department of Mechanical Engineering, Faculty of Engineering, Kafrelsheikh University, Kafrelsheikh 33156, Egypt

Keywords:

Coalbed methane
methane hydrate
micro-particles
hydration reaction kinetics

Cited as:

Wu, Q., Tang, T., Zhao, Z., Li, L., Elhefnawey, M., Zhang, B. Influence of micro-particles on gas hydrate formation kinetics: Potential application to methane storage and transportation. *Advances in Geo-Energy Research*, 2023, 10(3): 189-199.

<https://doi.org/10.46690/ager.2023.12.05>

Abstract:

Methane hydration is a safe, stable and environmentally friendly technology to bind and utilize excess coalbed methane gas. However, a limiting factor of the commercial application of coalbed methane hydration technology is the sluggish hydration reaction kinetics of methane hydrate formation, which needs to be improved. In this work, different micro-particle suspensions are prepared from an initial solution containing gellan gum and L-tryptophan, along with varying mass fractions of NiMnGa, Cu and carboxylated multi-walled carbon nanotubes, and their influence on the reaction kinetics in methane hydrate formation is examined. The results show that the formation of methane hydrate is enhanced by these micro-particles to varying degrees. Micro-particles show a synergistic solubilization effect with L-tryptophan and gellan gum at 6.2 MPa. The induction times of 1 wt.% NiMnGa system and 1 wt.% Cu system are the shortest. The 2 wt.% NiMnGa system has a pronounced impact on methane gas consumption, and the average gas consumption rates of the 0.1 wt.% Cu system and 1 wt.% NiMnGa system are faster. However, as the concentration of Cu micro-particles increases, both gas consumption and the average generation rate exhibits a linear decrease. This work offers valuable recommendations for choosing the experimental settings, micro-particle types and concentrations. We also lay the groundwork for the practical and sustainable application of coalbed methane storage and transportation technology employing the hydrate approach.

1. Introduction

Coalbed methane is an unconventional natural gas resource endowed in coal seams, with CH₄ as its main component (Asif et al., 2022; Gao et al., 2023). As a clean energy source with high calorific value and abundant reserves, coalbed methane has an important position and great potential in the energy field (Butalov and Klemes, 2011; Zhou et al., 2016; Jia et al., 2019). However, the utilization rate of coalbed methane in China is still under 50% (Zhang et al., 2021). Meanwhile, methane is also a potent greenhouse gas (Rochussen et al., 2023). On a time scale of 100 years, it has an about 34-fold air warming potential than the same amount of carbon dioxide (Myhre et al., 2013). Discharging coalbed methane directly into the

atmosphere is both a waste of energy and a great danger to the environment. Hence, expediting the storage, transportation and utilization of coalbed methane holds immense practical importance in augmenting the provision of environmentally advantageous energy and mitigating glasshouse gas emissions.

At present, gas storage and transport technology mainly includes gas liquefaction and compression (Lin et al., 2018; Wan et al., 2023). These systems necessitate liquefying the gas at a very low temperature (-160 °C) under harsh processing conditions (Qyyum et al., 2017; Veluswamy et al., 2018) and gas compression from 10 to 25 MPa for reactor storage, with inadequate safety and stability factors (McTaggart-Cowan et al., 2006; Mahboub et al., 2012). These limit the technology of storing and using coalbed methane. Wu et al. (2012)

proposed the hydrate-based coalbed methane storage and transfer technology in 2009. Methane hydrates are crystalline compounds that resemble ice and are created when methane and water combines under specific temperature and pressure. It has the characteristics of mild generation conditions (synthesis is possible at temperatures and pressures over 0 degrees Celsius), high gas storage rate (164 V/V compared to gas at standard temperatures and pressures), and safe storage (stable storage at atmospheric pressure and $-10\sim-15^{\circ}\text{C}$) (Englezos and Lee, 2005; Sum et al., 2009; Wang et al., 2009; Es-lamimanesh et al., 2012). Therefore, gas hydrate technology has potential application value in the field of coalbed methane storage and utilization. However, the efficiency of gas hydrate storage and transportation processes is significantly hindered by the mass and heat transfer properties exhibited by the gas-liquid phases. The traditional hydration enhancement methods can be categorized into physical and chemical methods. The physical methods mainly include spraying (Zhao et al., 2015), mechanical stirring (Meleshkin and Marasanov, 2021), bubbling (Cai et al., 2017), external magnetic field (English and Allen, 2019), electric field (Pahlavanzadeh et al., 2020), ultrasonic field (Park and Kim, 2013), and other methods. The chemical methods mainly encompass the addition of kinetic enhancers such as sodium dodecyl sulfate (SDS) (Zhang et al., 2023) and amino acids (Gaikwad et al., 2021; Yodpetch et al., 2023). These methods all act on a single liquid-phase structure and feature limited ability to promote the hydration reaction. In recent years, researchers revealed that the addition of nanoparticles with high specific surface area characteristics can be combined with accelerators, such that the single liquid phase becomes a liquid-solid two-phase structure. Based on these characteristics of large specific surface area and active Brownian motion, the gas-liquid contact area is increased, which achieves a strong promotion of the methane hydration mass transfer process and further improves its conditions (Arjang et al., 2013; Li et al., 2017; Montazeri et al., 2019).

Recently, research on nanoparticles focused on metal monomers, metal oxides, carbon nanomaterials, and ferromagnetic alloy micro-nanofluids. Functionalized multi-walled carbon nanotubes were tested for carbon dioxide hydrate kinetics and thermodynamics by Nashed et al. (2019). The experimental results demonstrated that the combination of carboxylated multi-walled carbon nanotubes (CNTs) and SDS increased the initial hydrate formation rate and gas absorption compared to the single SDS system. Furthermore, the hydrate self-preservation effect of the system was enhanced by the addition of CNTs at atmospheric pressure. Firoozabadi and Bonyadi (2020) found that the gas consumption and hydrate conversion rate of Fe_3O_4 and cetyltrimethylammonium bromide under the action of magnetic field increased by 200% compared with the system without a magnetic field, which indicated that optimizing the dispersion conditions of nanoparticles can significantly enhance the hydrate formation kinetics. Li et al. (2006) found that Cu nanoparticles can effectively enhance the heat and mass transfer process of HFC134a hydrate formation and increase the critical dissociation pressure of HFC134a hydrate at 9.5°C , thus improving the stable preservation conditions of hydrate. Wu et

al. (2023) discovered that NiMnGa (NMG) has stable phase-transition heat-absorption characteristics at 20 MPa and below, which can absorb the released heat during hydrate generation and significantly lower the temperature at the beginning of the growth phase, providing some subcooling conditions for hydrate generation to support hydrate generation. Yan et al. (2014) examined the storage, generation and induction of CH_4 hydrate in a solid n-tetradecane phase transformation material slurry using a semi-intermittent hydrator, and found that hydration peaked at 5.26 MPa and 158.7 V/V. Moreover, hydration took only 78 minutes. According to the review of relevant literature, nanoparticles and dispersants can improve the production of different hydrate solids. The above studies showed that the synergistic effect of nanoparticles and surfactants, combined with the perturbation of an external magnetic field, can enhance the gas hydration rate and increase the hydrate gas storage rate. However, nanoparticles have high surface energy and are prone to agglomeration, which prevents the maximization of the nanoparticle surface effect.

In summary, the local disturbance system presents the problems of limited influence area and high energy consumption, and the overall disturbance system of nanoparticles is burdened by particle agglomeration. This work analyzes and compares the effects of NMG, Cu and CNT particle types and concentrations on the formation kinetics of methane hydrate by adding the environmentally friendly kinetic promoters L-tryptophan and the physical dispersant gellan gum as the base solution, and further determines the best material addition ratio, providing some insights into the storage and transportation of methane.

2. Experiment

2.1 Materials

The metallic elements nickel (Ni), manganese (Mn) and gallium (Ga) were acquired from Zhongnuo New Materials (Beijing) Technology Co., Ltd. The reader is referred to the existing literature for detailed information on the production procedures about $\text{Ni}_{52.5}\text{Mn}_{22.5}\text{Ga}_{25}$ (Wu et al., 2022). The carboxylated multiwall carbon nanotubes (95%) were obtained from Nanjing Xianfeng Nanotechnology Co., Ltd. The CH_4 (99.9%) was sourced from Harbin Tongda Industrial Gas Co., Ltd. The water utilized for experimentation was purified class II water obtained by treatment with a Thermo Fisher Scientific water purifier.

2.2 Apparatus and calculation methods

Fig. 1 displays a schematic representation of the experimental configuration. The experimental setup modules and data processing procedures were detailed in previous works (Wu et al., 2022).

2.3 Experimental procedure

2.3.1 Preparation of the suspension

Suspensions containing different weight percentages, namely, 0, 0.1, 1, and 2 wt.%, of various particles (NMG, Cu, CNTs) were prepared. Then, 1 wt.% L-tryptophan and

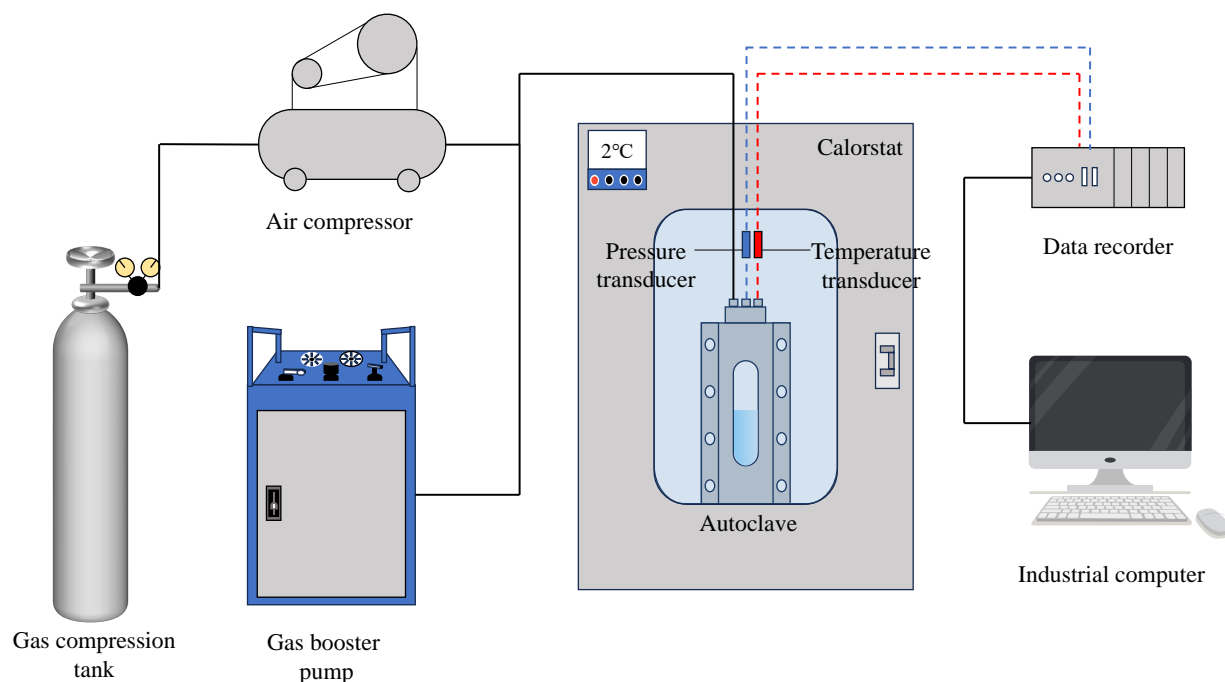


Fig. 1. Schematic of the static hydrate formation experimental setup.

Table 1. Composition of the different experimental systems.

System	Composition	Experiment	Particle (wt.%)
LG	L-Tryptophan + Gellan	LG	0
		LG + 0.1 wt.% NMG	0.1
LGN	L-Tryptophan + Gellan + NMG	LG + 1 wt.% NMG	1
		LG + 2 wt.% NMG	2
		LG + 0.1 wt.% Cu	0.1
LGC	L-Tryptophan + Gellan + Cu	LG + 1 wt.% Cu	1
		LG + 2 wt.% Cu	2
		LG + 0.1 wt.% CNTs	0.1
LGT	L-Tryptophan + Gellan + CNTs	LG + 1 wt.% CNTs	1
		LG + 2 wt.% CNTs	2

0.3 wt.% gellan gum were added to the 40 mL suspension. The suspension was dispersed using a high-speed shear mixer (S55, Vitamix) at a speed of 1,200 rad/min for 90 s. After dispersing, the reaction vessel was washed three times with pure water and dried for further use. The composition of the specific experimental systems tested is shown in Table 1.

2.3.2 CH₄ hydrate formation

Before the experiment, the gas-tightness of the experimental system was assessed by employing high-purity nitrogen gas. It was deemed excellent if the pressure within the reaction vessel exhibited a change of less than 0.1 MPa over two hours. Subsequently, the experiment was carried out in the following manner: The suspension within the reaction vessel

was hermetically sealed using a cover and linked to the gas inlet pipeline, temperature sensor and pressure sensor. The temperature of the system was kept at 2 °C through the manipulation of thermostatic chamber. Data on temperature and pressure were recorded at intervals of 10 seconds. After the system temperature had reached a stable state for one hour, methane (CH₄) was introduced into the vessel. To displace air within the reaction vessel, CH₄ at a pressure of 1 MPa was cycled three times. Subsequently, additional CH₄ was introduced into the reaction vessel until the initial pressure reached 6.2 MPa. The temporal interval commencing at $t = 0$ until the initial development of the primary hydrate crystal is commonly denoted as the induction period, which can be ascertained by examining the temperature-pressure distribution

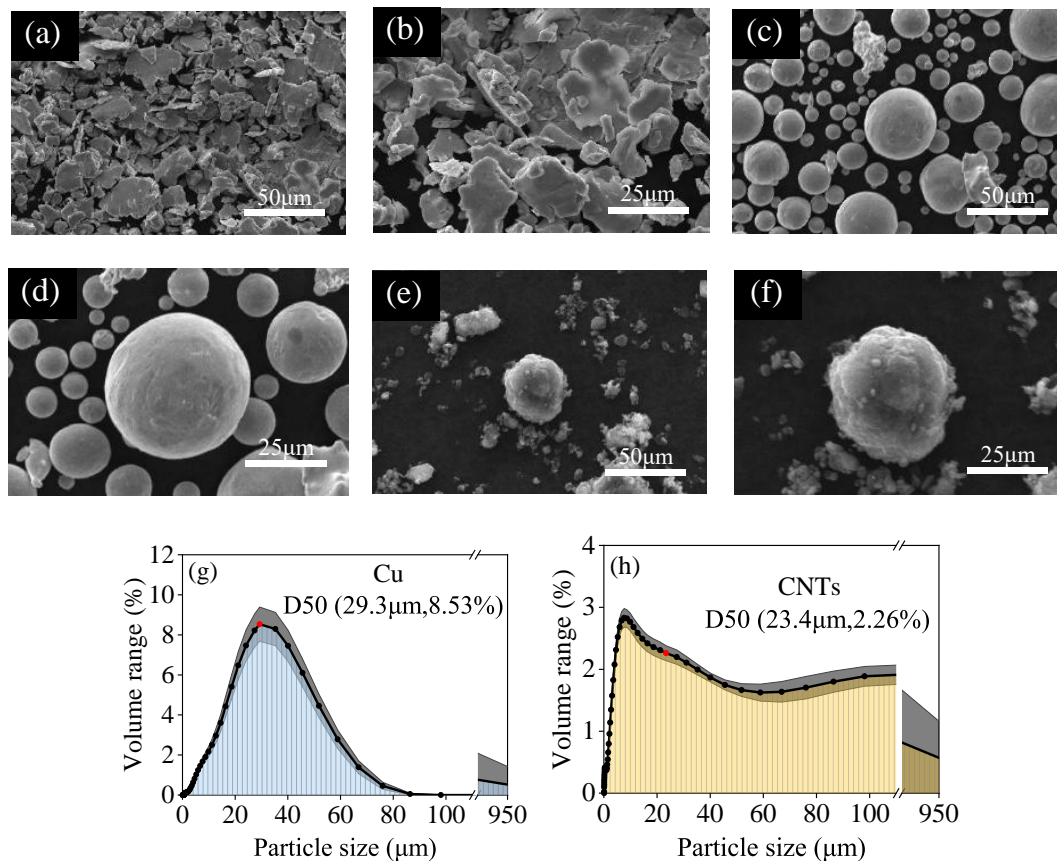


Fig. 2. Micro-particle surface morphology characteristics: (a) and (b) NMG, (c) and (d) Cu, (e) and (f). CNTs. Micro-particle size distribution: (g) Cu, (h) CNTs.

diagram. The completion of CH_4 hydrate synthesis was determined by observing a cessation in the system pressure decline, which remained stable for one hour. Next, the temperature was elevated to $30\text{ }^\circ\text{C}$ to induce the decomposition of the CH_4 hydrate, followed by expelling the gas present within the reaction vessel. The experimental procedures were replicated thrice for each of the experimental systems.

2.3.3 CH_4 solubility

In order to investigate the solubility of methane gas in different experimental solutions, the solubility measurement experiment of methane gas was carried out under the experimental conditions of $16\text{ }^\circ\text{C}$ and 6.2 MPa . The specific experimental steps were as follows:

- 1) Prior to the experiment, high-purity nitrogen gas was introduced into the reactor to test the airtightness of the experimental device. If the pressure change in the reaction vessel was less than 0.1 MPa within two hours, the experimental system's airtightness was considered acceptable.
- 2) The suspension was filled into the reactor and sealed. The temperature in the reactor was adjusted to $16\text{ }^\circ\text{C}$ by a thermostat, and the next operation could be carried out after 1 hour of stability.
- 3) Methane gas was injected into the reactor until 1 MPa was

reached to replace the air in the reactor. This operation was repeated three times.

- 4) Methane gas was injected into the reactor to 6.2 MPa , and the temperature and pressure data acquisition was started. When the temperature and pressure remained stable for 1 hour, the gas dissolution was completed.
- 5) The gas in the reactor was exhausted.

3. Results

3.1 Characterization

A FEI Quanta 250 scanning electron microscope was utilized to examine the microscopic morphological characteristics of the three types of micro-particles employed in this study. Previously, Wu et al. (2023) found that NMG alloy particles displayed irregular polygon forms in their exterior appearance, characterized by certain surfaces with a smooth, sawtooth-like texture. Figs. 2(c) and 2(d) illustrate the Cu micro-particles, exhibiting a spherical morphology characterized by many surface depressions. The Cu micro-particles demonstrated a notably greater specific surface area as compared to micro-particles of similar size. Figs. 2(e) and 2(f) depict the micro-particles of CNTs. When observed from a global standpoint, the CNT micro-particles had irregular forms. Furthermore, specific observations indicated the existence of a flocculent arrangement encompassing the particles, bearing resemblance

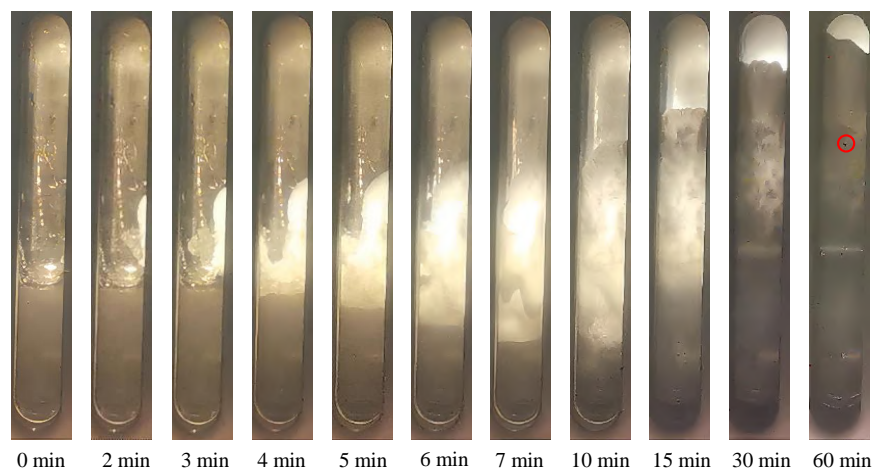


Fig. 3. Photos of the methane hydrate formation process in case-2.

to the visual characteristics of a “cotton candy” formation.

In order to analyze the particle size distribution characteristics of three types of micro-particles, a Malvern Mastersizer 3000E laser particle size analyzer was used to obtain the particle size distribution of NMG, Cu and CNTs. A previous study (Wu et al., 2022) showed the NMG particle size distribution, while Figs. 2(g) and 2(h) exhibit Cu and CNTs, respectively. NMG and Cu exhibited a normal distribution trend with relatively good distribution effects. On the other hand, the particle size distribution of CNTs displayed bimodal distribution, with a higher proportion of fine and coarse particles and a lower proportion of intermediate particles, indicating a more dispersed size distribution. The median diameter (D50) for the three types of micro-particles ranged from 18.7 to 29.3 μm , indicating that they exist in the same size range.

3.2 Methane hydrate formation kinetics

The present study investigates the kinetics of methane hydrate formation in the experimental systems of LG, LGN, LGC, and LGT, within a static hydrate formation setup. Experiments were conducted to generate methane hydrates by manipulating the concentration of micro-particles. Table 2 displays the experimental conditions and results of methane hydrate formation in the different micro-particle systems.

The morphology of hydrate generation provides valuable information on the mechanism of hydrate generation. The methane hydrate formation process of case-2 is shown in Fig. 3, corresponding to the hydrate growth pattern at different time points. Hydrate crystals are observed in the window for the first time at 2 min into the experiment, and methane hydrate grows along the window and the kettle wall in the early stage of the reaction. During 2-15 min, methane hydrate grows rapidly in the direction of both the gas and liquid phase space, covering 3/4 of the window in a short time, probably because of the presence of gas tunnelling between the hydrate and the kettle wall, promoting the rapid growth of hydrate in both directions (Ren et al., 2023). At the same time, it can be found that NMG particles migrate with the growth of hydrate in the

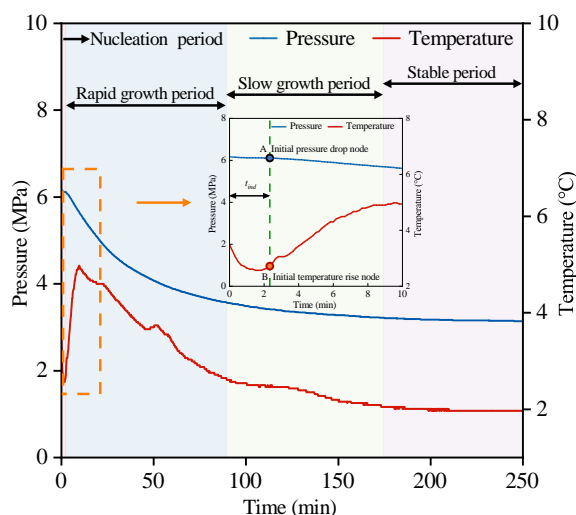
image at 60 min, which further increases the gas-liquid contact area and promotes the rapid growth of methane hydrate.

The process of methane hydrate formation can be categorized into two primary stages: Nucleation and growth. The characterization of the methane hydrate formation process in case-2 is depicted in Fig. 4. The nucleation stage in this experiment is described as the duration between the start of the experiment ($t = 0$) and the emergence of the first hydrate crystal (Kang et al., 2014). These crystals are considered critical hydrate nuclei, that is, with a critical size and stable properties. This period is commonly referred to as induction time (t_{ind}) and can be determined by analyzing the initial pressure drop node and the initial temperature rise node (indicated by the orange area in Fig. 4). The phenomenon wherein hydrate nuclei undergo stabilization and transform into solid hydrate crystals is commonly referred to as the growth phase. During the initial stage of this phase, the substantial driving force facilitates the migration of methane molecules from gas phase into “crystal cage” formed by the hydrogen bonding of water molecules in the liquid phase. This process is accompanied by a noticeable decrease in gas pressure, commonly referred to as the rapid hydrate growth stage (indicated by the blue area in Fig. 4). As time progresses, many methane gas molecules are sequestered into the “crystal cage”, the overpressure decreases and the rate of gas pressure decrease slows down, indicating that the hydrate reaction enters a slow-growth phase. When the gas pressure is close to the hydrate phase equilibrium pressure, the overpressure tends to zero and the methane gas molecules lack the enough driving force to enter the “crystal cage”. When the temperature and pressure of the system remain unchanged for 30 minutes, it indicates that the process of methane hydrate formation is over (indicated by the purple area in Fig. 4).

The solubility of methane gas is among the factors affecting the hydrate formation kinetics. Its values in different micro-particles systems is shown in Fig. 5: Pure water, LG, LG + 2 wt.% NMG, LG + 2 wt.% Cu, and LG + 2 wt.% CNTs, at 16 °C and 6.2 MPa. The solubility values obtained are as follows: 0.535, 0.715, 0.844, 0.787, and 0.802 $\text{mmol}\cdot\text{mol}^{-1}$, respectively. It is shown that the combination of gellan gum

Table 2. Experimental conditions and results of methane hydrate formation in the different systems.

Case	Experiment	Size (μm)	Particle (wt.-%)	Induction time (min)	Avg gas consumption (mmol/mol)	Gas consumption rate (mmol/(mol·min))	
						$V_{30\text{min}}$	V_{avg}
0	LG	-	0	2.5	40.706	0.710	0.176
1	LG + 0.1 wt.% NMG	18.7	0.1	2.28	42.253	0.795	0.190
2	LG + 1 wt.% NMG	18.7	1	1.72	43.029	0.815	0.207
3	LG + 2 wt.% NMG	18.7	2	2.17	43.830	0.783	0.195
4	LG + 0.1 wt.% Cu	37.5	0.1	2.22	42.990	0.837	0.215
5	LG + 1 wt.% Cu	37.5	1	1.78	42.060	0.777	0.181
6	LG + 2 wt.% Cu	37.5	2	2.72	41.605	0.808	0.178
7	LG + 0.1 wt.% CNTs	23.7	0.1	2.11	40.584	0.724	0.185
8	LG + 1 wt.% CNTs	23.7	1	2.33	41.981	0.687	0.159
9	LG + 2 wt.% CNTs	23.7	2	2	42.581	0.705	0.162

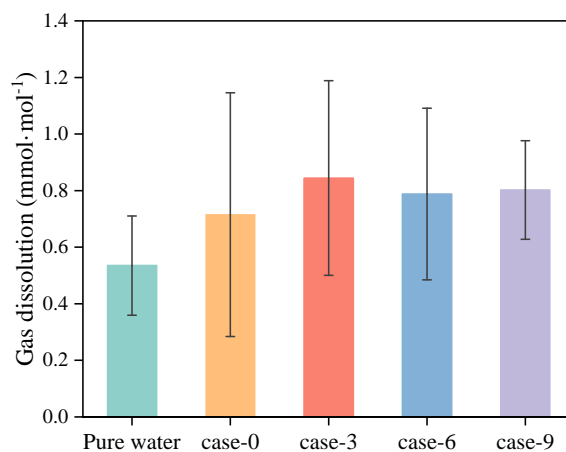
**Fig. 4.** Characteristic curve of temperature and pressure during hydrate formation in case-2.

and L-tryptophan is effective in solubilizing methane, while the addition of micro-particles further increases the methane solubility of the system. For example, in the LG system, LG + 2 wt.% NMG, LG + 2 wt.% Cu, and LG + 2 wt.% CNTs systems, the methane solubility is increased by 33.64%, 57.76%, 47.10%, and 49.91%, respectively, compared with that of the pure water system. The LG + 2 wt.% NMG system has the best effect on methane solubility.

4. Discussion

4.1 Induction time

Induction time is the main parameter for evaluating the rate of hydrate nucleation. The induction time for four distinct systems is shown in Fig. 6. Compared with the LG system, other than the LG + 2 wt.% Cu system, all systems exhibit further shortened induction time. The inclusion of micro-parti-

**Fig. 5.** CH_4 solubility in the different micro-particle systems at 16 °C and 6.2 MPa.

cles (NMG, Cu, CNTs) at 0.1 wt.% leads to a decrease in the induction time by 8.8%, 11.2% and 15.6%, respectively. When adding 1 wt.% micro-particles, it can be observed that the induction time is decreased by 31.2%, 28.8%, and 6.8%, respectively. Among them, LG + 1 wt.% NMG and LG + 1 wt.% Cu have a significant effect on the reduction of induction time. The incorporation of micro-particles at 2 wt.% leads to a decrease in the induction time by 13.2%, -8.8%, and 20.0%, respectively. The LG + 1 wt.% Cu system exhibits the most favorable outcome. In both the LGN and LGC systems, the induction time is shown to be influenced by the mass fraction of micro-particles, exhibiting the same change trends. The addition of particles at a mass fraction of 1 wt.% is found to be the most favorable scenario in terms of induction time reduction.

L-tryptophan, possessing a moderate level of hydrophobicity (hydrophobic index of -0.9) and an aromatic side chain, has been demonstrated to facilitate the formation of methane hydrate by augmenting the establishment of localized hydro-

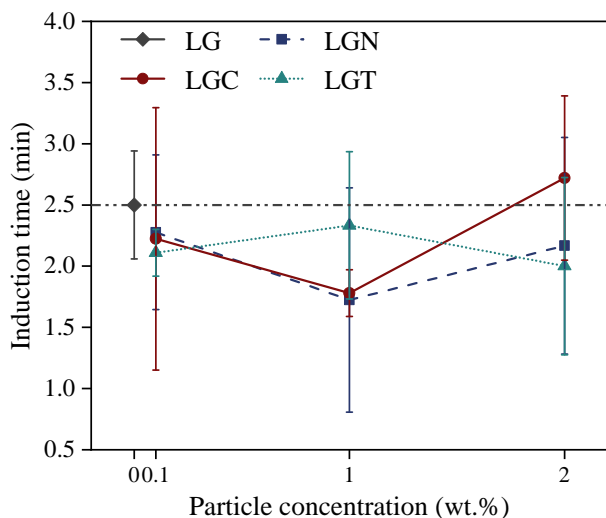


Fig. 6. Induction time of the different micro-particle systems.

gen bonds within water molecules (Kyte and Doolittle, 1982; Sa et al., 2013; Veluswamy et al., 2017). Furthermore, the micro-particles of NMG, Cu and CNTs have a large surface area, enlarging the contact interface between the gas and liquid phases and promoting the mass transfer progress during hydrate formation. Meanwhile, active Brownian motion, also exhibited by micro-particles, results in the generation of micro-convection that serves to diminish the stratospheric bottom layer. This phenomenon leads to an increase in turbulent intensity, facilitating the acceleration of heat transfer. This in turn substantially improves the overall thermal conductivity of the system, hence providing favorable experimental conditions for the production of hydrates (Li et al., 2017; Song et al., 2018). In addition, particle size also has an important effect on methane hydrate nucleation, as small-sized particles can provide more nucleation sites for hydrate nucleation (Li et al., 2021).

The present work aims to increase the kinetic process of methane hydrate production using a synergistic approach. This is achieved by mixing amino acids of environmentally friendly kinetic promoters with micro-particles. To weaken the aggregation characteristics of micro-particles in experimental systems, we utilize gellan gum as a dispersant for the micro-particle suspension. Nevertheless, in cases where the mass fraction of micro-particles surpasses the maximum load-bearing capacity of gellan gum, there is still a tendency for the partial aggregation and sedimentation of micro-particles to transpire. Therefore, selecting an appropriate concentration of micro-particles is of great significance for fundamental research on the kinetic process of hydrate formation.

4.2 Gas consumption

The evaluation of gas consumption serves as a crucial technical element of determining the conversion efficiency of hydrates and the capacity of natural gas hydrate storage and transportation technologies. The ultimate and temporal processes of gas consumption are illustrated in Figs. 7 and 8, respectively. It is evident that the LGN, LGC and LGT systems demonstrate a substantial rise in the ultimate consumption of

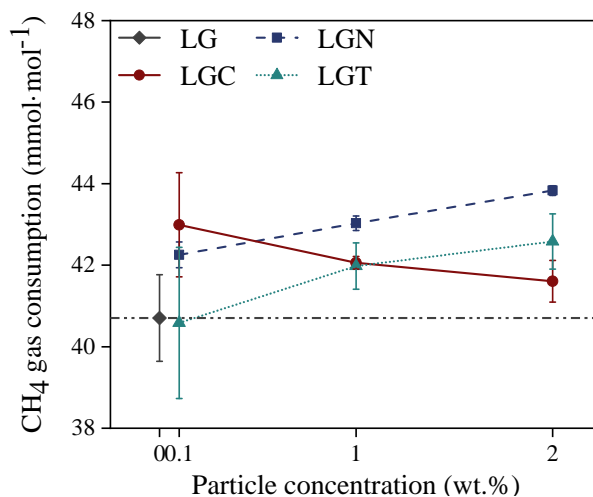


Fig. 7. CH₄ gas consumption in the different micro-particle systems.

CH₄ gas when compared to the LG system. In particular, the final utilization of CH₄ gas in LGN (NMG with concentrations of 0.1, 1 and 2 wt.%) exhibits respective increases of 3.80%, 5.71%, and 7.68%. In LGT (CNTs with concentrations of 0.1, 1 and 2 wt.%), the resultant consumption of CH₄ gas exhibits increases of 0.30%, 3.13% and 4.60%, respectively.

It can be seen that the correlation between the consumption of CH₄ gas in LGN and LGT and the concentration of micro-particles within the experimental concentration range is positive. The augmentation of the mass fraction of NMG and CNT micro-particles leads to a concurrent rise in the number of sites where methane hydrate nuclei can form. This increase in the formation sites facilitates more active Brownian motion among particles and expedites the transfer of energy within the reactor. Based on the findings presented in Fig. 7, the LG+1 wt.% Cu system demonstrates the highest gas consumption. This comprises a notable 5.61% increase in final CH₄ gas consumption compared to the LG system. The difference is merely 1.92% below the LG + 2 wt.% NMG system. Meanwhile, it is observed that when the mass fraction of Cu nanoparticles increases, there exists an inverse relationship between gas consumption and the concentration of Cu micro-particles in the LGC system within the specified experimental concentration range. In solutions with the same concentrations, particles with lower density exhibit a greater propensity for suspension, whereas particles with higher density tend to clump and settle. This leads to a reduction in the contributory impact of micro-fluids on mass and heat transfer.

4.3 Gas consumption rate

The gas consumption rate is a significant kinetic metric, which characterizes the rate at which gas hydrates form and plays a crucial role in evaluating their growth. When compared with the LG system, the average CH₄ gas consumption rate of CH₄ was observed to decrease by 9.66%, and 7.96% for LGT (1 and 2 wt.% CNTs), respectively (Fig. 9). In contrast, the average methane gas consumption rate of LGC (0.1, 1 and 2 wt.% Cu) exhibited respective increases of 22.10%, 2.84% and 1.14%.

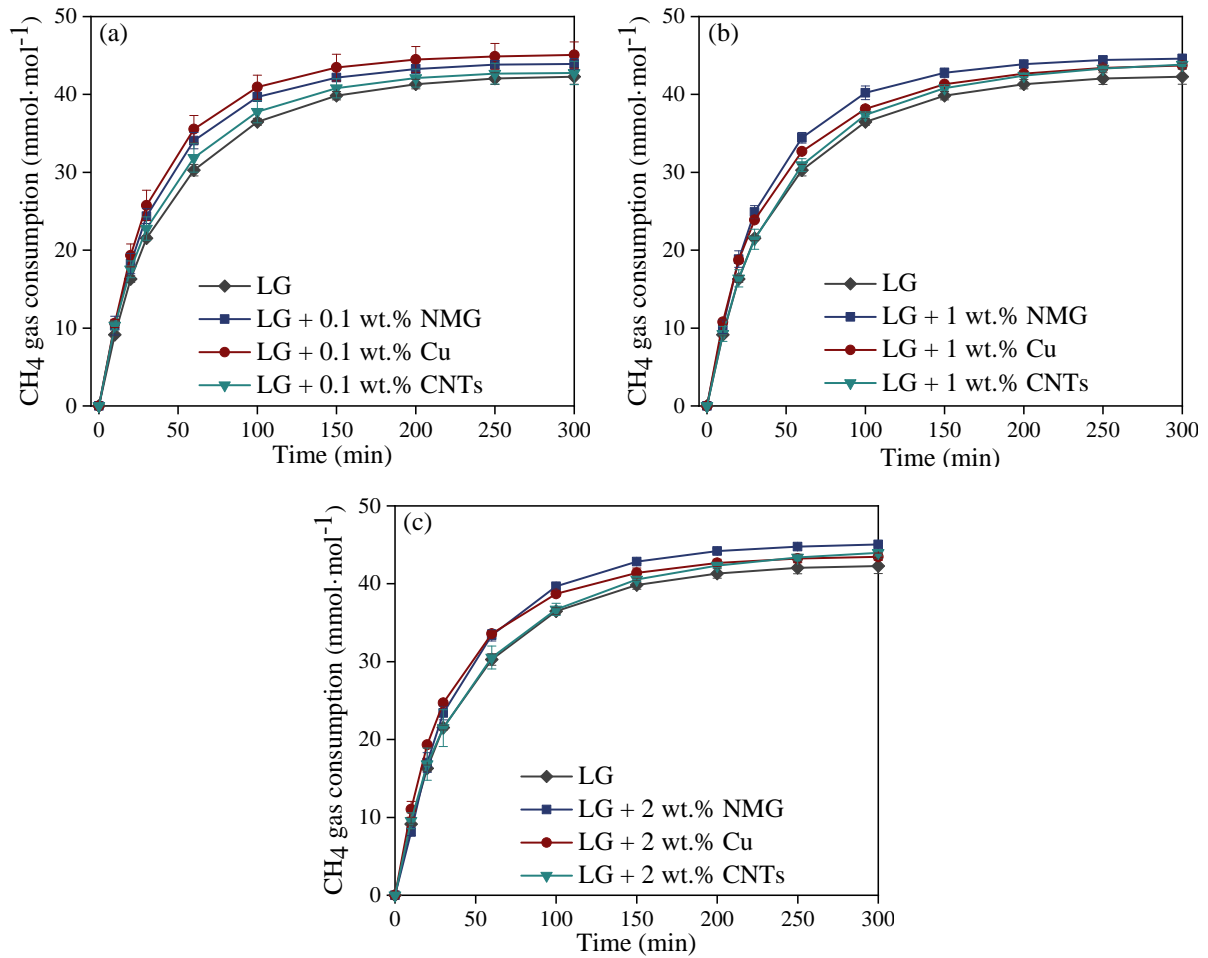


Fig. 8. Process curve of CH₄ gas consumption in the different micro-particle systems. (a) 0.1 wt.%, (b) 1 wt.%, (c) 2 wt.%.

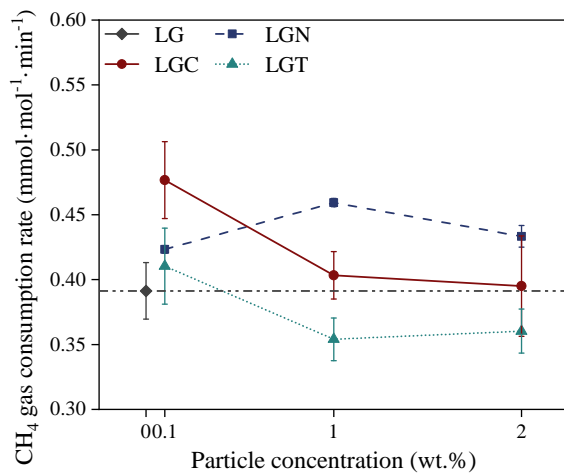


Fig. 9. CH₄ gas consumption rate of the different micro-particle systems.

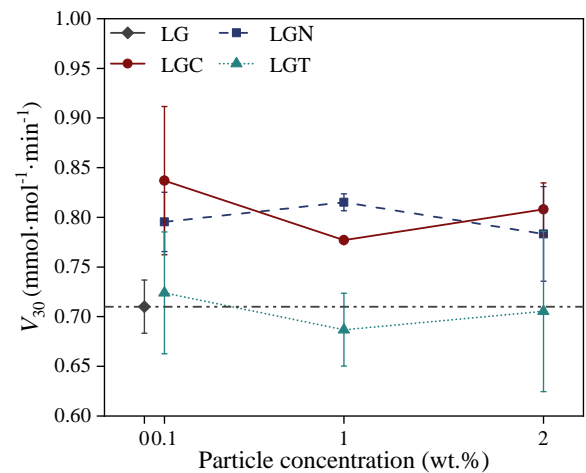


Fig. 10. CH₄ gas consumption rate in the first 30 minutes of the different micro-particle systems.

These data reveal a gradual decline in the average CH₄ gas consumption rate as the mass fraction of micro-particle increases in both the LGC and LGT systems. In the LGC system, with the increase in Cu mass fraction, the local particle distribution on the liquid phase surface becomes denser, exceed-

ing the limit of the cemented gel support, which directly affects the CH₄ gas consumption rate. Fig. 10 illustrates the trend of the average gas consumption rate with the concentration of micro-particles of LGC and LGT systems within the initial 30-minute period, exhibiting a notable rebound in

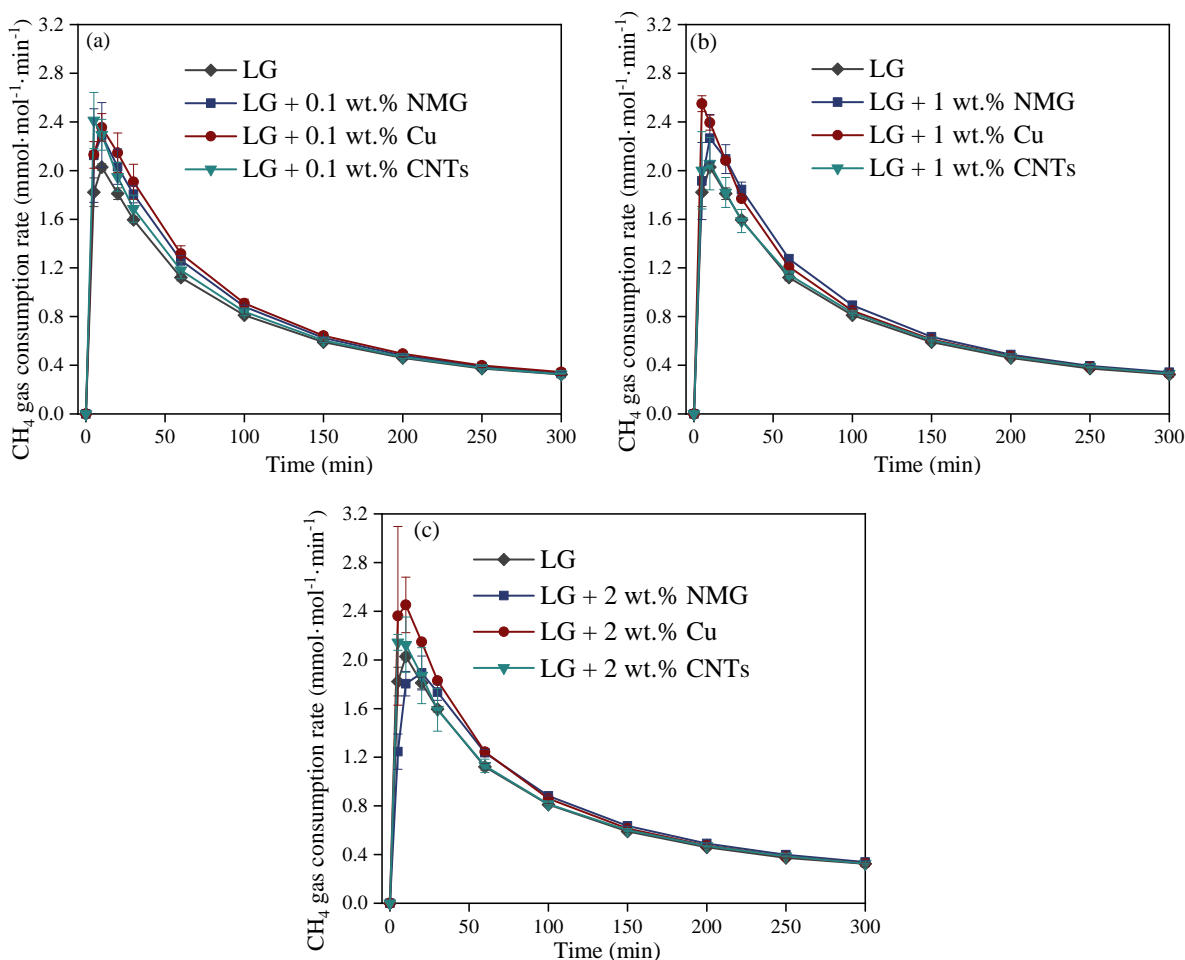


Fig. 11. Process curve of CH₄ gas consumption rate in the different micro-particle systems. (a) 0.1 wt.%, (b) 1 wt.%, (c) 2 wt.%.

contrast to the findings depicted in Fig. 9. This suggests that gellan gum exhibits the most effective support for Cu during the initial phase of the reaction, achieving an upward trajectory of the rate of CH₄ gas consumption.

The LGN system, at 1 wt.% and 2 wt.%, exhibits superior performance in enhancing the rate of methane hydrate formation when compared to other systems. The primary reason for this phenomenon can be attributed to the fact that NMG possesses the lowest particle size and demonstrates heat absorption characteristics during phase transitions. Furthermore, the presence of a sawtooth-shaped surface on NMG offers an elevated quantity of nucleation sites for the production of methane hydrates. The increase in nucleation sites improves the mass and heat transfer conditions, thereby promoting the formation of methane hydrate (Wu et al., 2023).

The real-time variation curves of the average CH₄ gas consumption rate for different micro-particle systems are displayed in Fig. 11. The LG + 1 wt.% Cu and LG + 2 wt.% Cu systems exhibit the most pronounced peak values of methane gas consumption rates within 10 minutes (Figs. 11(b) and 11(c)). These peak values are 2.549 mmol/(mol·min) and 2.452 mmol/(mol·min), respectively. Compared with the

LG system, it is observed that the methane gas consumption rates are increased by 25.690% and 20.907% respectively, suggesting that the addition of Cu micro-particles has a strong promotional influence on the rapid development stage of methane hydrate. If the suspension effect of Cu in the liquid phase can be further improved, the kinetics of methane hydrate formation will be further enhanced.

In this study, the compounding of L-tryptophan, gellan gum and micron particles obtained a synergistic effect in enhancing the methane hydrate generation kinetics, which further promoted the improvement of methane hydrate generation enhancement technology into a promising route for methane storage, transportation and utilization.

5. Conclusions

In this work, we investigated the methane hydrate formation characteristics in a self-built experimental system for visualizing gas hydrate crystallization in micro-fluids. We examined the influence of NMG, Cu, CNTs, and particle mass fraction on the methane hydrate formation characteristics. The results showed that, compared to the LG system without micro-particle additives, LGN and LGC effectively enhance

the kinetics of methane hydrate formation, while LGT has a moderate effect. From the viewpoint of methane gas solubility, L-tryptophan and gellan gum have a synergistic solubilizing effect when mixed with these three micromaterials. In terms of hydrate generation morphology, the growth of methane hydrate migrates the particles, further increasing the gas-liquid contact interface to promote methane hydrate generation. The systems of LG+1 wt.% NMG (1.72 min) and LG+1 wt.% Cu (1.78 min) have a significant impact on the shortening of induction time. The gas consumptions of LG+1 wt.% and 2 wt.% NMG are all above $43 \text{ mmol}\cdot\text{mol}^{-1}$, which is higher than other systems. In terms of the methane hydrate formation kinetics parameters, the optimal composition system is LG+1 wt.% NMG. Therefore, the LGN system further enhances the generation kinetics of methane hydrates under static conditions and is a potential promoter in the field of coalbed methane hydrate solidification storage and transportation. These findings provide some guidance into ways to further improve the utilization rate of coalbed methane.

Acknowledgements

This work was funded by the National Natural Science Foundation of China (Nos. U21A20111 and 51804105), the Fundamental Research Funds for the Central Universities (No. 3072022TS1005) and the Fundamental Scientific Research Funds of Provincial Universities in Heilongjiang Province (No. 2022-KYYWF-0530).

Conflict of interest

The authors declare no competing interest.

Open Access This article is distributed under the terms and conditions of the Creative Commons Attribution (CC BY-NC-ND) license, which permits unrestricted use, distribution, and reproduction in any medium, provided the original work is properly cited.

References

- Arjang, S., Manteghian, M., Mohammadi, A. Effect of synthesized silver nanoparticles in promoting methane hydrate formation at 4.7 MPa and 5.7 MPa. *Chemical Engineering Research and Design*, 2013, 91: 1050-1054.
- Asif, M., Wang, L., Wang, R., et al. Mechanisms in CO₂-enhanced coalbed methane recovery process. *Advances in Geo-Energy Research*, 2022, 6(6): 531-534.
- Butalov, I., Klemes, J. J. Clean fuel technologies and clean and reliable energy: A summary. *Clean Technologies and Environmental Policy*, 2011, 13: 543-546.
- Cai, J., Xu, C., Xia, Z., et al. Hydrate-based methane separation from coal mine methane gas mixture by bubbling using the scale-up equipment. *Applied Energy*, 2017, 204: 1526-1534.
- Englezos, P., Lee, J. D. Gas hydrates: A cleaner source of energy and opportunity for innovative technologies. *Korean Journal of Chemical Engineering*, 2005, 22: 671-681.
- English, N. J., Allen, C. C. R. Magnetic-field effects on methane-hydrate kinetics and potential geo-physical implications: Insights from non-equilibrium molecular dynamics. *Science of The Total Environment*, 2019, 661: 664-669.
- Eslamimanesh, A., Mohammadi, A. H., Richon, D., et al. Application of gas hydrate formation in separation processes: A review of experimental studies. *The Journal of Chemical Thermodynamics*, 2012, 46: 62-71.
- Firoozabadi, S. R., Bonyadi, M. A comparative study on the effects of Fe₃O₄ nanofluid, SDS and CTAB aqueous solutions on the CO₂ hydrate formation. *Journal of Molecular Liquids*, 2020, 300: 112251.
- Gaikwad, N., Sangwai, J. S., Kumar, R., et al. CO₂-CH₄ hydrate formation using l-tryptophan and cyclooctane employing a conventional stirred tank reactor. *Energy & Fuels*, 2021, 35(16): 13224-13239.
- Gao, Q., Hou, B., Zhao, J., et al. Coalbed methane hydrate separation: An experimental study using ordered mesoporous materials. *Industrial & Engineering Chemistry Research*, 2023, 62(12): 4864-4874.
- Jia, D., Qiu, Y., Li, C., et al. Propagation of pressure drop in coalbed methane reservoir during drainage stage. *Advances in Geo-Energy Research*, 2019, 3(4): 387-395.
- Kang, S. P., Shin, J. Y., Lim, J. S., et al. Experimental measurement of the induction time of natural gas hydrate and its prediction with polymeric kinetic inhibitor. *Chemical Engineering Science*, 2014, 116: 817-823.
- Kyte, J., Doolittle R. F. A simple method for displaying the hydropathic character of a protein. *Journal of Molecular Biology*, 1982, 157(1): 105-132.
- Li, J., Liang, D., Guo, K., et al. Formation and dissociation of HFC134a gas hydrate in nano-copper suspension. *Energy Conversion and Management*, 2006, 47(2): 201-210.
- Li, D., Peng, H., Liang, D. Thermal conductivity enhancement of clathrate hydrate with nanoparticles. *International Journal of Heat and Mass Transfer*, 2017, 104: 566-573.
- Li, Y., Wu, N., He, C., et al. Nucleation probability and memory effect of methane-propane mixed gas hydrate. *Fuel*, 2021, 291: 120103.
- Lin, W., Xu, J., Gao, T., et al. Analysis of heat transfer irreversibility in processes for liquefaction of coalbed methane with nitrogen. *Industrial & Engineering Chemistry Research*, 2018, 57(17): 5895-5902.
- Mahboub, M. J. D., Ahmadpour, A., Rashidi, H. Improving methane storage on wet activated carbons at various amount of water. *Journal of Fuel Chemistry and Technology*, 2012, 40(4): 384-389.
- McTaggart-Cowan, G., Reynolds, C., Bushe, W. Natural gas fuelling for heavy-duty on-road use: Current trends and future direction. *International Journal of Environmental Studies*, 2006, 63(4): 421-440.
- Meleshkin, A. V., Marasanov, N. V. Study of enhancement of synthesis of freon 134a gas hydrate during boiling of liquefied gas with its simultaneous stirring with water. *Journal of Engineering Thermophysics*, 2021, 30: 699-703.
- Montazeri, V., Rahimi, M., Zarenezhad, B. Energy saving in carbon dioxide hydrate formation process using boehmite nanoparticles. *Korean Journal of Chemical Engineering*, 2019, 36: 1859-1868.

- Myhre, G., Shindell, D., Pongratz, J., et al. Anthropogenic and natural radiative forcing, in *Climate Change 2013: The Physical Science Basis*, edited by G. Myhre et al., Cambridge University Press, Cambridge, pp. 659-740, 2013.
- Nashed, O., Partoon, B., Lal, B., et al. Investigation of functionalized carbon nanotubes' performance on carbon dioxide hydrate formation. *Energy*, 2019, 174: 602-610.
- Pahlavanzadeh, H., Hejazi, S., Manteghian, M. Hydrate formation under static and pulsed electric fields. *Journal of Natural Gas Science and Engineering*, 2020, 77: 103232.
- Park, S. S., Kim, N. J. Study on methane hydrate formation using ultrasonic waves. *Journal of Industrial and Engineering Chemistry*, 2013, 19(5): 1668-1672.
- Qyyum, M. A., Qadeer, K., Lee, M., et al. Comprehensive review of the design optimization of natural gas liquefaction processes: Current status and perspectives. *Industrial & Engineering Chemistry Research*, 2017, 57(17): 5819-5844.
- Ren, J., Zeng, S., Chen, D., et al. Roles of montmorillonite clay on the kinetics and morphology of CO₂ hydrate in hydrate-based CO₂ sequestration. *Applied Energy*, 2023, 340: 120997.
- Rochussen, J., Jaeger, N. S. B., Penner, H., et al. Development and demonstration of strategies for GHG and methane slip reduction from dual-fuel natural gas coastal vessels. *Fuel*, 2023, 349: 128433.
- Sa, J. H., Kwak, G. H., Lee, B. R., et al. Hydrophobic amino acids as a new class of kinetic inhibitors for gas hydrate formation. *Scientific Reports*, 2013, 3: 2428.
- Song, Y., Wang, F., Guo, G., et al. Energy-efficient storage of methane in the formed hydrates with metal nanoparticles-grafted carbon nanotubes as promoter. *Applied Energy*, 2018, 224: 175-183.
- Sum, A. K., Koh, C. A., Sloan, E. D. Clathrate hydrates: From laboratory science to engineering practice. *Industrial & Engineering Chemistry Research*, 2009, 48(16): 7457-7465.
- Veluswamy, H. P., Kumar, A., Seo, Y., et al. A review of solidified natural gas (SNG) technology for gas storage via clathrate hydrates. *Applied Energy*, 2018, 216: 262-285.
- Veluswamy, H. P., Lee, P. Y., Premasinghe, K., et al. Effect of biofriendly amino acids on the kinetics of methane hydrate formation and dissociation. *Industrial & Engineering Chemistry Research*, 2017, 56(21): 6145-6154.
- Wan, M., Ji, W., Wan, J., et al. Compressed air energy storage in salt caverns in China: Development and outlook. *Advances in Geo-Energy Research*, 2023, 9(1): 54-67.
- Wang, W., Carter, B. O., Bray, C. L., et al. Reversible methane storage in a polymer-supported semi-clathrate hydrate at ambient temperature and pressure. *Chemistry of Materials*, 2009, 21(16): 3810-3815.
- Wu, Q., Li, Z., Chen, F., et al. Ferromagnetic shape memory alloy Ni₅₂·5Mn₂₂·5Ga₂₅: Phase transformation at high pressure and effects on natural gas hydration. *Materials Letters*, 2023, 343: 134371.
- Wu, Q., Lin, N., Li, L., et al. Experimental study on the kinetics of the natural gas hydration process with a NiMnGa micro-nanofluid in a static suspension system. *Water*, 2022, 14(5): 745-745.
- Wu, Q., Zhang, Q., Zhang, B., et al. Influence of super-absorbent polymer on the growth rate of gas hydrate. *Safety Science*, 2012, 50(4): 865-868.
- Yan, H., Song, X., Xin, F., et al. Storage capacity and duration of methane hydration in a slurry of solid n-tetradecane. *Energy & Fuels*, 2014, 29(1): 130-136.
- Yodpetch, V., Inkong, K., Veluswamy, H. P., et al. Investigation on the amino acid-assisted CO₂ hydrates: A promising step toward hydrate-based decarbonization. *ACS Sustainable Chemistry & Engineering*, 2023, 11(7): 2797-2809.
- Zhang, X., Zhao, J., Chen, C., et al. SDS-promoted methane hydrate growth in presence of a superhydrophobic substrate. *Chemical Engineering Science*, 2023, 276: 118761.
- Zhang, Q., Zhen, J., Zhang, B., et al. Coal mine gas separation of methane via clathrate hydrate process aided by tetrahydrofuran and amino acids. *Applied Energy*, 2021, 287: 116576.
- Zhao, J., Tian, Y., Zhao, Y., et al. Experimental investigation of effect on hydrate formation in spray reactor. *Journal of Chemistry*, 2015, 2015: 261473.
- Zhou, F., Xia, T., Wang, X., et al. Recent developments in coal mine methane extraction and utilization in China: A review. *Journal of Natural Gas Science and Engineering*, 2016, 31: 437-458.